The hydrophobic effect and its role in cold denaturation ☆

Cristiano L. Dias [a,*], Tapio Ala-Nissila [b,c], Jirasak Wong-ekkabut [a], Ilpo Vattulainen [c,d,e], Martin Grant [f], Mikko Karttunen [a]

[a] Department of Applied Mathematics, The University of Western Ontario, Middlesex College, 1151 Richmond St. N., London, Ont., Canada N6A 5B7
[b] Department of Physics, Brown University, Providence, RI 02912-1843, USA
[c] COMP Center of Excellence and Department of Applied Physics, Helsinki University of Technology, P.O. Box 1100, FI-02015 TKK, Espoo, Finland
[d] Institute of Physics, Tampere University of Technology, P.O. Box 692, FI-33101 Tampere, Finland
[e] MEMPHYS-Center for Biomembrane Physics, University of Southern Denmark, Denmark
[f] Physics Department, Rutherford Building, McGill University, 3600 rue University, Montŕeal, Que., Canada H3A 2T8

ARTICLE INFO

ABSTRACT

The hydrophobic effect is considered the main driving force for protein folding and plays an important role in the stability of those biomolecules. Cold denaturation, where the native state of the protein loses its stability upon cooling, is also attributed to this effect. It is therefore not surprising that a lot of effort has been spent in understanding this phenomenon. Despite these efforts, many unresolved fundamental aspects remain. In this paper we review and summarize the thermodynamics of proteins, the hydrophobic effect and cold denaturation. We start by accounting for these phenomena macroscopically then move to their atomic-level description. We hope this review will help the reader gain insights into the role played by the hydrophobic effect in cold denaturation.

© 2009 Elsevier Inc. All rights reserved.

Introduction

Using cold temperatures in biology and medicine has its origins in ancient Egypt where they were used for healing already around 2500 BC. The birth of modern cryobiology is often associated with James Arnott (1797–1883) who applied cold temperatures to destroy cancerous tumors [20]. The temperatures he reached were not extreme by today's standards, only to −24 °C, but his work has been the inspiration for using cold temperatures as a cheap and efficient method for certain surgical operations as well as for preservation of biological matter. In today's cryotherapy, liquid nitrogen temperatures are typically applied.

At a more microscopic level, temperature is one of the most important parameters in defining proteins' behavior in living matter. It is now well established that proteins denature at both high (typically ∼60 °C) and low (typically ∼−20 °C) temperatures [40,58,57]. The term 'denaturation' typically refers to the well established phenomenon of heat denaturation, whereas the latter is often called 'cold denaturation' and it is the focus of this article. Denaturation can also be induced by pressure [34,46].

Denaturation, by heat or cooling, refers to the loss of the unique three-dimensional structure [3] a protein has under physiological conditions. When a protein experiences this structural instability it also loses its functionality. Although cold denaturation has been experimentally established [57,59] and even suggested to be a universal mechanism present in most proteins [42,52,57], it is much harder to study experimentally due to the necessary sub-zero temperatures. When considering cold denaturation as a universal mechanism, two notable exceptions should be noticed. First, despite several studies, there is only one report of cold denaturation in hyperthermophile organisms [16]. Second, the so-called 'intrinsically disordered proteins' are known to be resistant against heat denaturation and experiments have now shown that to be the case for their low temperature behavior as well although the kinetic mechanisms may be different [1]. Historically, cold denaturation (in the presence of urea) was first suggested by Hopkins in 1930 [33].

Non-covalent bonding (i.e., hydrogen bonds, electrostatic interactions and hydrophobicity) plays a crucial role in the structural stability of proteins. Hydrogen bonding is important for the formation of secondary structures, while electrostatic and hydrophobic interactions are needed for stabilizing the tertiary structure of proteins. The subtle variation in the relative strengths of these interactions lies in the heart of denaturation. Nowadays it is clear that understanding hydrophobicity [15,24] and the role of entropy vs. enthalpy [23] are key for a better understanding. However, fundamental questions remain unanswered despite several theoretical

modeling and computer simulations at lattice and even atomistic levels [10,12,17,19,23,45,47,54,61,70].

In our earlier work [23], we introduced a microscopic model to describe heat and cold denaturation within the same framework. Clathrate cages (particular order structures of water molecules) around non-polar residues were identified as the crucial structure leading to both types of denaturation. Their high entropic cost accounts for the folding of the protein at ambient temperature while their low enthalpy is responsible for the unfolding of the protein at low temperature. This explains why cold denaturation proceeds with heat release as opposed to heat absorption seen during heat denaturation. Notice that a literal interpretation of the word "cage" calls for caution since a complete hydrate cage around the solute is likely to form at only low temperature while at ambient temperature only incomplete cages survive for a reasonable amount of time. In this paper we summarize some of the theoretical efforts to understand microscopically the hydrophobic effect and the role it plays in cold denaturation. We proceed as follow: in the next section we describe the thermodynamics of proteins and identify the hydrophobic effect as the main mechanism behind cold denaturation. This effect is discussed in "Hydrophobic effect". Thermodynamical and atomic models accounting for cold denaturation are introduced in "Cold denaturation", providing an explanation for the phenomena. A conclusion is given at the end.

Thermodynamics of proteins

In their natural environment proteins exist in a variety of configurations, which can be mapped into folded and unfolded states of the protein [21]. In equilibrium, the stability of a configuration associated with the folded structure is given by the relative free energy of these two states [40,58,71]: $\Delta G = G^u - G^f$. The folded state is stable if $\Delta G > 0$, and this stability increases with increasing ΔG. If $\Delta G < 0$, then the system unfolds spontaneously, releasing energy to the environment. Thermodynamics provides a framework for describing the temperature dependence of ΔG [6]. This dependence is obtained by expanding the enthalpy and the entropy around the transition point by means of the heat capacity as described below.

At the transition temperature T_c, both the folded and unfolded configurations have the same energy:

$$\Delta G(T_c) = \Delta H(T_c) - T_c \Delta S(T_c) = 0, \qquad (1)$$

such that

$$\Delta S(T_c) = \Delta H(T_c)/T_c, \qquad (2)$$

where ΔS is the change in entropy and ΔH is the change in enthalpy. The enthalpy of transition can be written in terms of the heat capacity at constant pressure:

$$\Delta H(T) = \Delta H(T_c) + \int_{T_c}^{T} dT\, \Delta C_P(T), \qquad (3)$$

since $\Delta C_p \equiv (\partial \Delta H(T)/\partial T)_p$. Whenever $\Delta C_P(T)$ can be considered to be constant, this equation reduces to:

$$\Delta H(T) = \Delta H(T_c) + (T - T_c)\Delta C_P. \qquad (4)$$

For the entropy of transition, we have

$$\Delta S(T) = \Delta S(T_c) + \int_{T_c}^{T} dT\, (\partial \Delta S(T)/\partial T)$$
$$= \frac{\Delta H(T_c)}{T_c} + \int_{T_c}^{T} d(\ln T)\, \Delta C_P(T) = \frac{\Delta H(T_c)}{T_c} + \Delta C_P \ln\left(\frac{T}{T_c}\right), \qquad (5)$$

where the last equality is obtained by assuming that ΔC_p is constant.

Now, by considering Eqs. (4) and (5) together, we obtain the Gibbs energy of unfolding:

$$\Delta G(T) = \Delta H(T) - T\Delta S(T)$$
$$= \frac{(T_c - T)}{T_c}\Delta H(T_c) + (T - T_c)\Delta C_P - T\Delta C_p \ln\left(\frac{T}{T_c}\right). \qquad (6)$$

This equation brings about that the temperature dependence of ΔG is determined by T_c, $\Delta H(T_c)$, and ΔC_P. These quantities can be obtained experimentally from calorimetry experiments [57], which have shown *typical* numbers for real proteins to be [63]: $T_c = 60\,°C$, $\Delta H(T_c) = 500\,kJ\,mol^{-1}$, and $\Delta C_P = 10\,kJ\,mol^{-1}\,K^{-1}$.

Fig. 1 shows the temperature dependence of ΔG for a *typical* protein. This quantity has a convex shape, indicating the presence of two phase transitions. These transitions take place whenever $\Delta G(T) = 0$. The transitions correspond to *heat denaturation* at $T = T_c$, and to *cold denaturation* at $T \simeq -30\,°C$. At intermediate temperatures, between $T \simeq -30\,°C$ and T_c, the folded configuration is thermodynamically stable, with maximal stability occurring at about $17\,°C$. It is interesting to note that even under most stable conditions, very little energy is required to unfold the protein: $\Delta G(T = 17\,°C) \simeq 32\,kJ\,mol^{-1}$. Thus, while nature requires the folded protein to be stable in order to function, the stability is marginal, with $32\,kJ\,mol^{-1}$ being only a minor fraction (about 5%) of the interaction energy of a single covalent bond between two carbon atoms.

In this work, we are mainly interested in the low temperature transition to the denatured state, i.e., cold denaturation. Thermodynamically this transition results from the convex curvature of the Gibbs energy. This curvature can be computed from Eq. (6):

$$\frac{\partial^2 \Delta G(T)}{\partial T^2} = -\frac{\Delta C_P}{T}, \qquad (7)$$

and it becomes convex, i.e., $\partial^2 \Delta G(T)\partial T^2 < 0$, whenever $\Delta C_p > 0$. For globular proteins ΔC_p is positive [57] and increases with the length of the protein [43]. This feature is mostly attributed to the hydration of non-polar amino acids which have a distinguishable positive ΔC_p, as opposed to polar amino acids that contribute negatively to the heat capacity of proteins [36,56].

The temperature T_d at which cold denaturation occurs can be obtained by solving $\Delta G(T_d) = 0$. This task becomes a simple analytical exercise when the logarithmic term in Eq. (6) is approximated by its second order Taylor expansion:

$$\ln\left(\frac{T_c}{T}\right) \simeq \left(\frac{T_c - T}{T}\right) - \frac{T_c - T}{2T^2}. \qquad (8)$$

The temperature at which cold denaturation takes place then reads [40]:

$$T_d^2 \simeq \frac{T_c^2 \Delta C_p}{2\Delta H(T_c) + T_c \Delta C_p}. \qquad (9)$$

This equation shows clearly that cold denaturation becomes accessible at higher temperatures for proteins with larger ΔC_p and T_c. Notice that $\Delta H(T_c)$ has the opposite effect on T_d.

For a *typical* protein, the temperature at which cold denaturation occurs is below the freezing point of water, see Fig. 1. This undesirable feature for experimental studies is usually overcome by weakening the folded protein through pressure [40,46,59,68] or chemical denaturants [37,57]. Qualitatively, the weakening can be seen as shifting of the convex Gibbs energy (shown in Fig. 1) downwards, thereby increasing T_d above freezing, and decreasing T_c. Pressure has the additional effect of decreasing the freezing point of water to $-22\,°C$ (at 200 MPa) such that experiments can be performed within a wider range of temperatures below $0\,°C$. The drawback of using pressure or chemistry to weaken
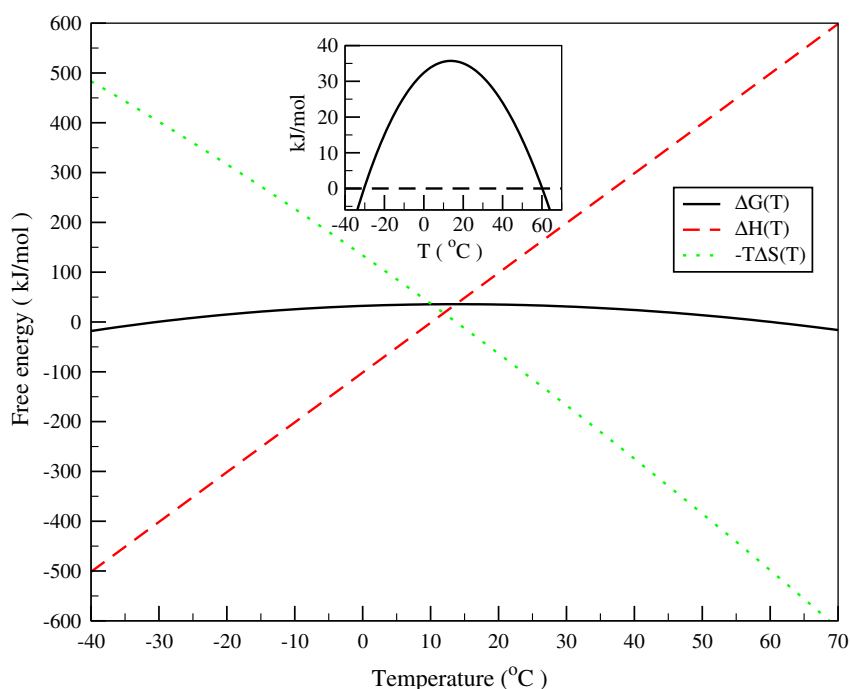
Fig. 1. Temperature dependence of the Gibbs free energy $\Delta G(T)$, entropic energy $-T\Delta S(T)$ and enthalpy $\Delta H(T)$ of folding of a typical protein. Inset shows zoom of the Gibbs free energy of folding. T_c and T_d are the temperatures at which heat and cold denaturation occur, respectively.

the protein is that it becomes difficult to deconvolute the effect of those denaturants from cold denaturation itself.

In Table 1 we show the experimental value of T_d for a few selected proteins. Notice that the actual value of T_d is strongly dependent on the experimental technique used to weaken the stability of a protein.

Summarizing, cold denaturation in globular proteins takes place because of their large positive heat capacity of unfolding. This is related to the hydration of non-polar residues and thus to the hydrophobic effect, which we discuss in the next section. It is important to realize since the hydrophobic effect is a general property of globular proteins [24,35], cold denaturation is also expected to be a general phenomenon. However, the interpretation of cold denaturation calls for some caution, since it is technically difficult to observe and differentiate the related phenomena. For example, experimental data have recently reported cold denaturation in a hyperthermophile protein [16]. Meanwhile, due to the lack of folded structure, intrinsically disordered proteins do not lose solubility either at high or low temperatures [1].

Table 1
Experimental temperature for cold (T_d) and heat (T_c) denaturation.

	T_d (°C)	T_c (°C)
Chymotrypsinogen pH 2.07 (0.3 GPa) [32][a]	−9	49
Ribonuclease pH 2 (0.3 GPa) [32][a]	−32	30
Ubiquitin pH 4.0 (0.2 GPa) [37]	−12	82
Metmyoglobin pH 3.84 [57][b,c]	7	55
Metmyoglobin pH 3.70 [57][b,c]	10	44
Apomyoglobin pH 4.70 [57][b,c]	1	51
Apomyoglobin pH 4.78 [57][b,c]	−3	54
Staphylococcal nuclease pH 6.0 [57][b,c]	6	33
Staphylococcal nuclease pH 6.5 [57][b,c]	4	38
Staphylococcal nuclease pH/p^{2}H 5.5 (0.15 GPa) [53][a]	0	48
B state of ferricytochrome c pH 13 [39][d]	−16	16

[a] Estimated from figures by Smeller [68].
[b] Estimated from figures by us.
[c] At ambient pressure.
[d] In the presence of NaCl: 0.01 M. Data for other concentrations of NaCl is also given by the authors.

Hydrophobic effect

The hydrophobic effect is one of the main driving forces for the formation of self-assembled biological structures such as lipid membranes and proteins [25]. It reflects the tendency of water to avoid non-polar molecular structures such as hydrocarbons and hydrophobic amino acids. The hydrophobic effect is largely due to the special ability of water molecules to form hydrogen bonds (H-bonds) with themselves, attempting to avoid structural arrangements where the network of these H-bonds is perturbed. Non-polar molecules such as lipids and hydrophobic amino acids thus tend to aggregate and displace themselves from contact with water.

The hydrophobic effect can be inferred from the Gibbs energy of transfer of non-polar molecules from their bulk liquid state into water: $\Delta G = G^{\text{water}} - G^{\text{bulk}}$. If ΔG is positive, then the solute prefers to be surrounded by other solutes as opposed to water. The larger ΔG becomes, the higher is the tendency of solutes to cluster together. In contrast, negative ΔG implies a molecule that is soluble in water.

Non-polar molecules have a large positive energy of transfer. For example, the free energy of transfer of methane molecules at 25 °C is about 26.2 kJ mol^{-1} [60]. Some insight can be gained by computing the enthalpy ΔH and entropy ΔS of transfer. For methane, the enthalpic contribution to ΔG is negative (-4.3 kJ mol^{-1}), while the entropic contribution $-T\Delta S$ is positive (28.7 kJ mol^{-1}) and corresponds to 85% of the interaction. Thus, the hydration of non-polar solutes is characterized by a small favorable enthalpy and a strong unfavorable entropy. The temperature dependences of ΔG, ΔH, and $-T\Delta S$ for methane are shown in Fig. 2. As temperature decreases, bulk methane becomes less stable since ΔG decreases. Enthalpy can be held responsible for this destabilization as ΔH decreases with decreasing temperature. Entropy has the opposite behavior, it stabilizes bulk methane since $-T\Delta S$ increases with decreasing temperature.

The effects of hydrophobicity can also be measured by the heat capacity of transfer from liquid to water via $\Delta C_p = C_p^{\text{water}} - C_p^{\text{bulk}}$. For
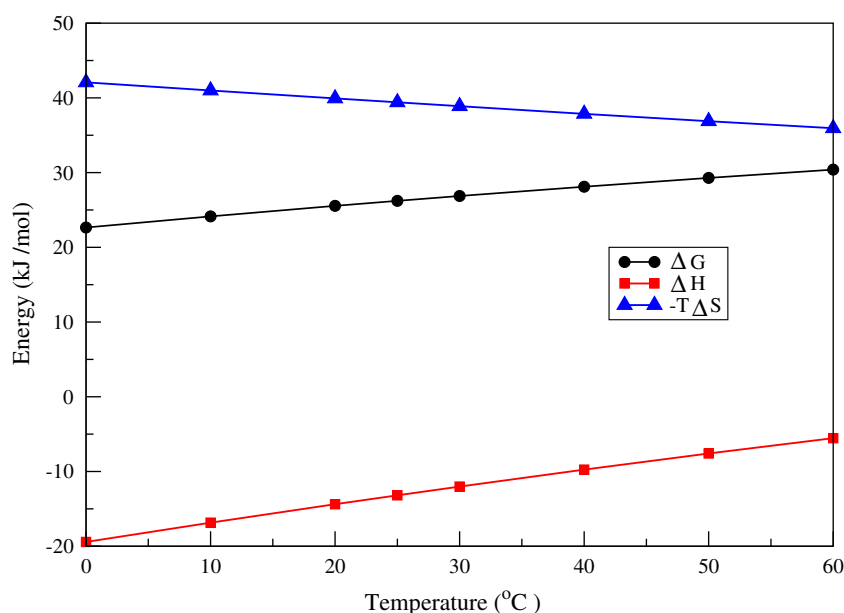
Fig. 2. Experimental data [60] of methane's free energy (circles), entropy (triangles) and enthalpy (squares).

simple solutions ΔC_p is small, while for non-polar solutes it is large and positive [27]. This large heat capacity of transfer has been shown to be proportional to the surface area around non-polar solutes accessible to water [44], and thus proportional to the number of solvent molecules around the solute [31].

Thermodynamics

As mentioned above the hydration of non-polar solutes in water has a large entropic cost and a small favorable enthalpy. This peculiar partition of the free energy imposes constraints on models for the hydrophobic effect. In this section we discuss a model introduced by Muller [31,41,50] that displays the correct partition of the free energy and provides insights into the microscopic nature of the phenomena due to its simplicity.

The focus of Muller's model is in the H-bond between water molecules. Those are assumed to exist in two states in mutual equilibrium:

$$Hbond(intact) \rightleftharpoons Hbond(broken), \qquad (10)$$
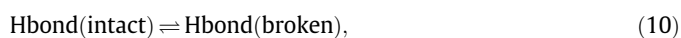
where the equilibrium constant K is given by:

$$K \equiv \frac{f}{1-f} = \exp(-\Delta G^\circ/RT). \qquad (11)$$

In this equation, f is the fraction of broken H-bonds, R is the gas constant and ΔG° is the difference in Gibbs free energy between broken and intact states ($\Delta G^\circ = G^{broken} - G^{intact}$). Based on the assumption that the energy of the system is determined by H-bonds alone, the enthalpy and entropy are given by:

$$H = fH^{broken} + (1-f)H^{intact}, \qquad (12)$$
$$S = fS^{broken} + (1-f)S^{intact}, \qquad (13)$$

and the specific heat is given by:

$$c_p \equiv \left(\frac{\partial H}{\partial T}\right)_P = \left(\frac{\partial f}{\partial T}\right)_P \Delta H^\circ. \qquad (14)$$

Here, $\Delta H^\circ \equiv H^{broken} - H^{intact}$ and it is assumed to be temperature independent. The dependence of f on temperature is obtained from Eq. (11):

$$\left(\frac{\partial f}{\partial T}\right)_P = \Delta H^\circ \frac{f(1-f)}{RT^2}, \qquad (15)$$

such that the specific heat [31] is given by:

$$c_p = (\Delta H^\circ)^2 f(1-f)/RT^2. \qquad (16)$$

Eqs. (12), (13) and (16) account for the enthalpy, entropy and specific heat of the H-bond network of water. Now, Muller assumes that hydration energies of non-polar solutes are related to rearrangements in this network alone. Thus hydration energies are computed as the difference in energies between the disturbed and undisturbed networks. Notice that the H-bond network is only perturbed locally by the solute, i.e., in the first hydrated shell, and only these molecules need to be taken into account for the hydration energies. This implies that f, ΔH° and ΔS° are different for bulk and first-shell water and we use b and s subscripts to distinguish them. Therefore the enthalpy and entropy upon hydration are given by:

$$\Delta H = n\left[(1-f_b)\Delta H_b^\circ - (1-f_s)\Delta H_s^\circ\right], \qquad (17)$$
$$\Delta S = n\left[(1-f_b)\Delta S_b^\circ - (1-f_s)\Delta S_s^\circ - R\Delta F\right], \qquad (18)$$

where $\Delta F = F_s - F_b$ with $F_b \equiv f_b \ln f_b + (1-f_b)\ln(1-f_b)$ and similarly for F_s. These are the "mixing" entropies characteristic of mixture models. In these equations, n is the number of H-bonds in the first-shell and it is related to number N of water molecules by $n = 3N/2$.[1] In the same line of thought the heat capacity of hydration is given by:

$$\Delta C_p^{hydration} = n\left[c_p^s - c_p^b\right], \qquad (19)$$

where c_p^s and c_p^b are the specific heat, given in Eq. (16), of first-shell and bulk water.

Actual values for the parameters of the model are given in Fig. 3. The entropy predicted with those values for propane, butane, and isobutane at 25 °C are −88.4 (−75.32), −101.4 (−93.20) and −98.9 (−89.14), respectively. Units are in J/K mol^{-1} and experi-

---

[1] To obtain Eq. (17), Muller assumes that the enthalpies of a broken H-bond in the first-shell and in the bulk are the same [41]. The same assumption is also made for the entropy of a broken H-bond in Eq. (18).
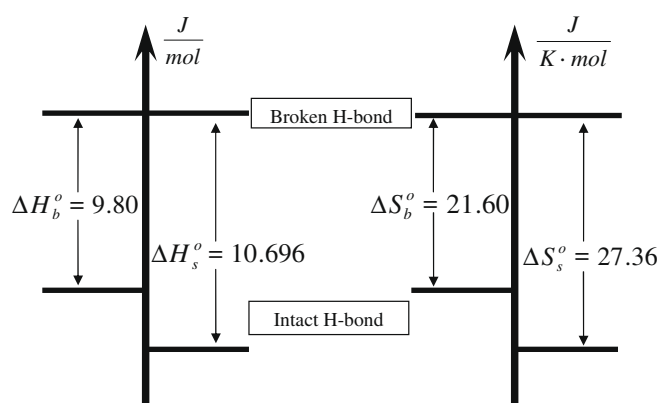
Fig. 3. Parameters for Muller's model. For the number N of water molecules in the first-shell Muller uses [31]: 25 for propane, 28 for butane and isobutane.

mental results are given in parentheses – showing a good agreement. The temperature dependence of the specific heat of hydration, Eq. (19), is characteristic of two-state models. It satisfactorily reproduces the positive $\Delta C^{\text{hydration}}$ for non-polar solute and the observed decrease in $\Delta C^{\text{hydration}}$ with increasing T [31].

Muller's model has been refined [41]. However, the original version of the model already shows that the energetic states of H-bonds are predominantly responsible for the thermodynamical features of the hydrophobic effect. The drawback of the model is that it requires many parameters and does not explain how the different energetic states of H-bonds correlate with the atomic structure of water.

Atomic description

The first "pictorial representation" of the hydrophobic effect came from Frank and Evans in 1945 [30]. While studying non-polar molecules in liquids, they computed anomalous negative entropy of mixing for aqueous solution. This implied that hydration of non-polar molecules increased the amount of order in the system.
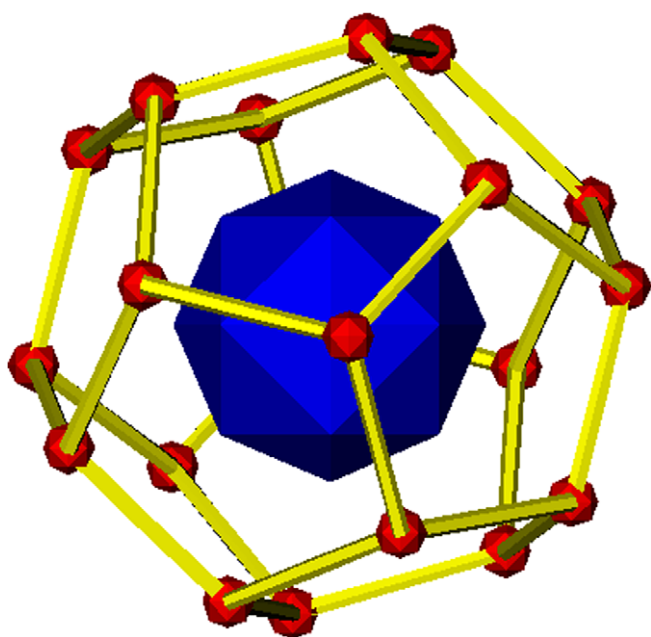

Fig. 4. Schematic representation of a clathrate hydrate caging a non-polar solute. Water molecules are in the vertices of the dodecahedron.

Also the expected positive heat of mixing related to an increase in the number of broken H-bonds in shell water was absent. Thus, they concluded that non-polar solutes perturbed water towards its crystalline state, locally ordering water and increasing the amount of H-bonds. Those ordered regions were named "iceberg", although it was noted that the name should not be taken literally.

The structure of water molecules in the iceberg region is still a question of debate. It is clear that icebergs account for much less order than ice and thus, the suggested name is misleading. This can be seen [35] by comparing the entropy released during freezing and during hydration per water molecule. Those are 22.17 J/K mol^{-1} and 4.18 J/K mol^{-1}, respectively. The latter is much smaller indicating that freezing brings water molecules to a much more ordered state then iceberg water. On the other hand, the amount of order in the icebergs is greater than in bulk (by 4.18 J/K mol^{-1} per water molecule).

Insights into the "iceberg" structure can be gained by looking at the distribution of H-bonds around the solute. At room temperature, water saturates 3–3.5 H-bonds with neighboring molecules. When a non-polar solute is inserted in water, the number of saturated H-bonds should be much smaller for the molecules in the first hydrated shell around the solute. This can see by fixing the position of a shell-water and rotating it in all possible orientations. In most of those orientations shell-water has at least one H-bond pointing towards the inert solute, therefore being non-saturated. On the other hand, a few orientations exist where all the H-bonds are saturated. We will refer to these two types of situations, as non-saturated and saturated ones.

Energy wise, the saturated orientations have a lower (more favorable) enthalpy than the many non-saturated ones. However, they also have lower (less favorable) entropy since there are not many of them. This shows a balance between enthalpy and entropy when the system switches from saturated to non-saturated orientations. This balance does not even out and the free energy of the system is smaller whenever shell-water are constrained to saturated orientations. In other words, the surface of the solute, which is tiled with water molecules, has saturated orientations as its tiling motif. Different types of tilings are possible. Those are called clathrate cages [9,29] and the simplest of them is represented by a dodecahedron with water molecules sitting on each of its vertex (see Fig. 4). It is likely that a perfect cage only occurs at low temperature and at room temperature only incomplete cages survive for a reasonable amount of time.

Thus, the formation of clathrate cages around the solute minimizes the free energy of shell water. However, even in those configurations shell-water has a higher free energy than bulk water, i.e., the hydration free energy is positive. Therefore, when more than one solute is inserted in water they tend to cluster to reduce the amount of shell water in the system. This occurs through the overlap of iceberg regions. The tendency of non-polar solutes to cluster is knows as the *hydrophobic interaction*. Since shell water are more ordered and form more H-bonds than bulk water, the clustering of solutes increases the entropy and enthalpy of the system. Therefore, the hydrophobic interaction is stabilized by entropy and destabilized by enthalpy. It is said to be entropically driven.

The behavior of the hydrophobic interaction upon cooling is of significance to this paper. For most materials, the average strength of the interaction between atoms increases as thermal energy decreases. In contrast, the strength of the hydrophobic interaction decreases with decreasing temperature. This non-intuitive behavior is related to the complex interplay between entropy and enthalpy – see Fig. 2. Upon cooling, both the stabilizing effect of entropy and the destabilizing effect of enthalpy increase. This indicates that the differentiation between shell and bulk water increases with decreasing temperature, with shell water becoming more ordered and forming more H-bonds than bulk water. However, the entropic

and enthalpic terms do not change at the same rate. The enthalpic penalty increases faster upon cooling, thus accounting for a weakening of the hydrophobic interaction. It should be noted that the interplay between enthalpy and entropy is not clearly understood from a microscopic point of view.

Cold denaturation

In the previous section we have discussed the thermodynamics of the hydrophobic effect and how it arises from the atomic structure of water. This effect has been shown to be the dominant driving force for protein folding and is responsible for the stability of the protein core [24,35,51]. It has been incorporated in simple models of proteins where the solvent is describe implicitly – an example is the well known Hydrophobic-Polar model [14]. An implicit description is unlikely to account for both cold and heat denaturation – unless the parameters in the model are made temperature dependent [17]. When the solvent is described explicitly both heat and cold denaturation are recovered naturally [4,10,11,13,18,19,23,54,55,61,62,65]. In the proceeding paragraphs an overview of two approaches used to mimic the hydrophobic effect in proteins through an explicit solvent are summarized. Explicitly, a thermodynamical approach based on Muller's model for water and a molecular dynamics approach based on a simple model that accounts for the relevant structure of shell water.

Thermodynamical model

One of the first models to account for cold denaturation in the physics literature was proposed by De Los Rios and Caldarelli [62]. In this model, the protein corresponds to a self-avoiding random walk where each amino acid occupies a site in a lattice. All other nodes i are occupied by water molecules which can be in the bulk or form the first shell around the polymer. The bulk state is considered to be q times degenerate and for simplicity the energy of this state is set to zero. The first shell can be in an ordered or a disordered state [50]. The disordered state is considered to be $q - 1$ times degenerate while the ordered state is not degenerate. This model is therefore described by three parameters: J, K and q.

– where J and K are the energies of the ordered and disordered shell states, respectively. If s describes the state of first shell water molecules such that $s = 0$ represents the ordered state and $s = 1, \ldots, q - 1$ corresponds to the disordered states, then the Hamiltonian is given by:

$$\mathscr{H} = \sum_j \left(-J\delta_{s_j,0} + K(1 - \delta_{s_j,0}) \right), \tag{20}$$

where the sum is over all water molecules that are nearest neighbors of some hydrophobic monomer. Therefore, for each conformation C of the polymer its energy can be computed. The partition function of the system can be cast in the form: $Z_N = \sum_C Z_N(C)$, where the partition function of a given conformation C is given by:

$$Z_N(C) = q^{n_b(C)}[\exp(\beta J) + (q - 1)exp(-\beta K)]^{n_s(C)}, \tag{21}$$

where n_s and n_b are the number of water molecules in the first shell and bulk, respectively, and β is reciprocal of the thermal energy.

It is possible to classify the polymer according to n_s. For self-avoiding random walks of size N, the fraction of configurations of perimeter n_s is well approximated by a Poisson distribution:

$$P_N(n_s) \sim e^{\delta(N-1)} \frac{[\delta(N-1)]^{2N+2-n_s}}{(2N+2-n_s)!}, \tag{22}$$

with $\delta \sim 0.75$. Using this distribution and Eq. (21), the partition function of the system reads:

$$Z_N(\beta) = \sum_{n_{min}}^{2N+2} P_N(n)q^{2N+2-n}[\exp(\beta J) + (q - 1)\exp(-\beta K)]^n, \tag{23}$$

where the smallest perimeter $n_{min} = 2\sqrt{\pi N}$, assuming that in this configuration the system has a circular compact shape. The maximum number of water sites in contact with the polymer is $2N + 2$. The heat capacity, computed as:

$$C_v = \beta^2 (\partial^2 \ln Z / \partial \beta^2), \tag{24}$$

is shown in Fig. 5. Three peaks appear in the heat capacity. From zero temperature to the first peak, the polymer is swollen – in agreement with cold denaturation. As the temperature is raised above the first peak, the polymer folds and the number of first shell water is approximately $2\sqrt{\pi N}$. As temperature increases above the
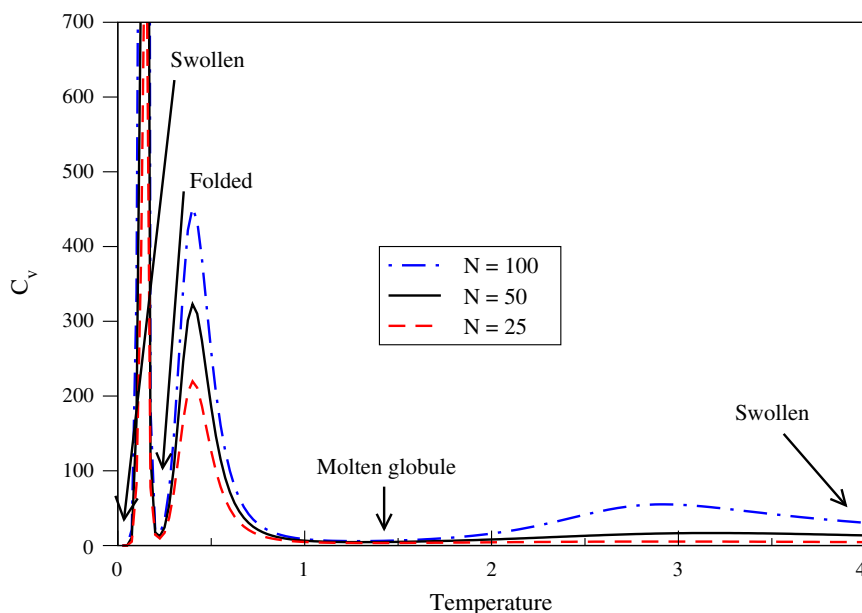

Fig. 5. Heat capacity, Eq. (24), for different polymer sizes. Here, $K/J = 2$ and $q = 10^3$.
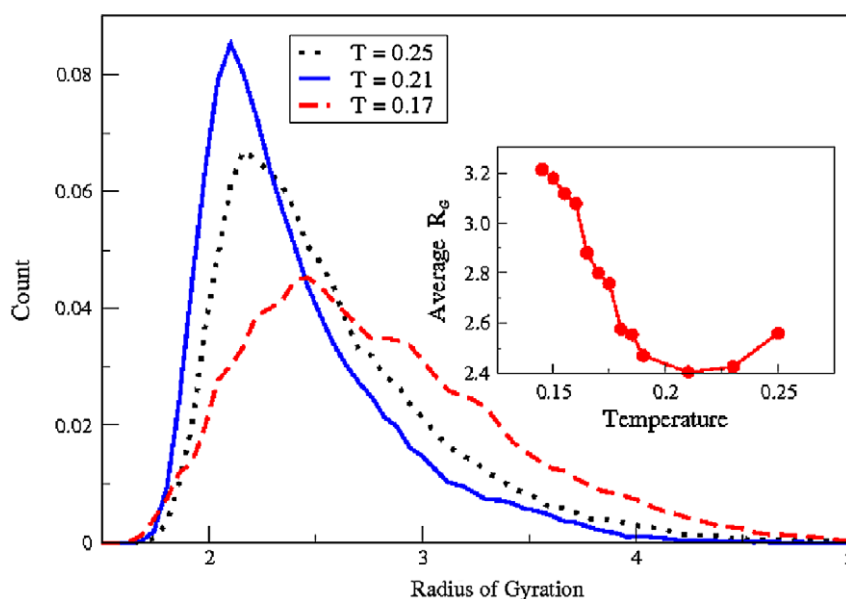
Fig. 6. Normalized distribution of the radius of gyration of the protein (R_G) at three effective temperatures: $T = 0.25$ ("hot" water), $T = 0.21$ (intermediate temperature) and $T = 0.17$ ("cold" water). Inset shows the detailed temperature dependence of the size of the protein [23].

second peak, the polymer occupies globule-molten states. Beyond the third peak, the polymer reopens.

Consistent with experiments, the free energy of the model has a convex curvature which is correctly partitioned in entropy and enthalpy [62]. The model has been extended successfully to study the presence of kosmotropes and chaotropes cosolvent [48,49]. However, as in the case of Muller's model, it does not provide much insight into the structure of water around the solute. In the next section we describe an attempt to fill this gap.

Atomic description

Recently, an effort to understand the physical mechanism behind cold denaturation of biopolymers was undertaken by constructing a minimal microscopic model for the protein–water system [23]. For computational efficiency, this study was performed in 2D. The water phase was modeled using the 2D Mercedes-Benz (MB) model [5,7,25] where H_2O molecules are represented as 2D disks, with three H-bonding arms resembling the famous Mercedes-Benz symbol. This model has now been extended to 3D and the first results look very promising [8,22]. This simple model (2D) reproduces many important thermodynamic properties of water, such as the density anomaly, the minimum in the isothermal compressibility as a function of temperature, the large heat capacity, and the experimental trends for the thermodynamic properties of hydration of non-polar solutes [25,67]. In the study, the parameters of the MB model were chosen to be those used by Silverstein et al. [66].

To model the protein, the simple bead-spring model of polymers [26] was used: monomers which are adjacent along the backbone of the protein are connected to each other by harmonic springs, and non-adjacent monomers are connected by a shifted Lennard-Jones potential. The interaction between monomers and water molecules was also given by a shifted Lennard-Jones potential with the same binding energy as between the water molecules.

To study the process of cold denaturation at constant pressure, molecular dynamics simulations were performed on the water–protein model system in the isothermal-isobaric ensemble [2,28,38]. The pressure in the system was set such that the MB model reproduces water-like anomalies seen at ambient pressure

[25] and hydrates non-polar molecules in a realistic manner [69]. Typically, the simulation box contained 512 molecules comprised of a 10-monomer long protein and 502 water molecules. To induce denaturation, simulations were performed at various different (effective) temperatures.

The main result for the study can be seen in Fig. 6, where the equilibrium distribution of the size of the protein, as measured by its radius of gyration R_G [26], is shown at three different temperatures. In "hot" water (referring to the largest values of T shown here), proteins favor more compact configurations with decreasing temperature. However, a further decrease of temperature results in reversal of this trend: as the temperature decreases further, the peak shifts to a *larger* value indicating that in "cold" water proteins become less compact for decreasing temperature. This behavior can be seen systematically in the inset of Fig. 6, which depicts the temperature dependence of the protein size. This type of non-monotonic behavior is characteristic to denaturation of real proteins and in line with previous studies [40,54,61].

Characteristic configurations of the protein at different temperatures are shown in Fig. 7. In cold water (upper panels), the monomers are surrounded by an ordered layer of "shell" water molecules. Molecules forming this cage are strongly H-bonded to each other and therefore have a low energy. At $T = 0.21$, the protein favors compact configurations. Water molecules close to the protein have at least one non-saturated H-bond which is pointing towards the protein. When the temperature is increased to $T = 0.25$, most monomers are in contact with the solvent. In Ref. [23], these observations were further quantified by computing the average H-bond energy per water molecule for shell and bulk water.

The molecular dynamics simulations of the MB model provide a simple microscopic picture for cold denaturation in terms of changes in hydration: at low temperatures water molecules infiltrate the folded protein in order to passivate the "dangling" water–water H-bonds found in shell water. At the same time, hydrophobic contacts are destabilized and an ordered layer of "shell" water molecules forms around the protein monomers such that they become separated by a layer of solvent in the cold denatured state. Solvent layers around the monomer pairs are highly ordered such that their formation decreases the total entropy of the
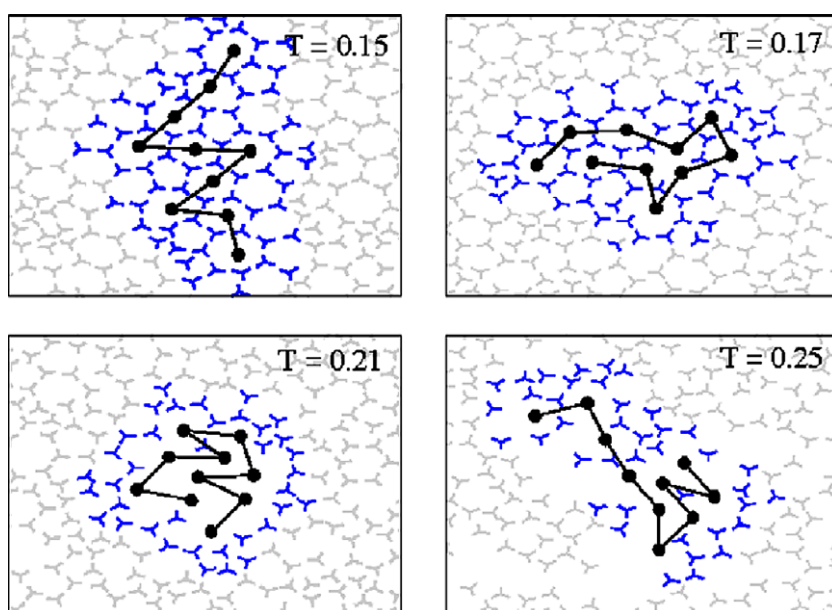
Fig. 7. Characteristic configurations of a protein in cold water ($T = 0.15$ and $T = 0.17$), at an intermediate temperature ($T = 0.21$), and in hot water ($T = 0.25$). The "shell" water molecules close to the protein are highlighted here. In cold water, the monomers are typically surrounded by clathrate-like cages [23].

system. The existence of such low entropic states for shell water at low T explains why cold denaturation proceeds with heat release as opposed to heat absorption seen during heat denaturation.

Conclusion

In this paper we reviewed and summarized some of the efforts to model and understand the hydrophobic effect and the role it plays in the thermodynamics of proteins. This review is not intended to be exhaustive but to focus on the recent advances in physics and chemistry, and especially on the efforts in computational modeling and theory. Thermodynamical models for the hydration of non-polar solutes are successful in reproducing experimental data accurately but they rely on many parameters that need to be adjusted (see "Thermodynamics"). They provide a basis for inferring the molecular structure of water around those solutes which is responsible for the hydrophobic effect (see "Atomic description" in "Thermodynamics of proteins"). When those thermodynamical models are coupled to a coarse-grained structure of proteins (see "Thermodynamical model"), non-trivial but realistic phases of these biomolecules are found to coexist. Simulations of simple models have been performed revealing a potential mechanism for cold denaturation of proteins which is consistent with the thermodynamical models (see "Atomic description" in "Cold denaturation"). Finally, when comparing with experiments, there are also subtleties which should be considered. For example, recent results have shown that replacing water with deuterium, as is common practise, may lead to changes in the physical properties [64].

Acknowledgments

References

[1] Agnes Tantos, P.T. Peter Friedrich, Cold stability of intrinsically disordered proteins, FEBS Lett. 583 (2009) 465.
[2] H.C. Andersen, Molecular dynamics simulations at constant pressure and/or temperature, J. Chem. Phys. 72 (1980) 2384.
[3] C.B. Anfinsen, Principles that govern the folding of protein chains, Science 181 (4096) (1973) 223–230.
[4] E. Ascolese, G. Graziano, On the cold denaturation of globular proteins, Chem. Phys. Lett. 467 (2008) 150–153.
[5] J.-P. Becker, O. Collet, Mercedes-Benz model of neutral amino-acid side chains, J. Mol. Struct.: THEOCHEM 774 (2006) 23–28.
[6] W.J. Becktel, J.A. Schellman, Protein stability curves, Biopolymers 26 (1987) 1859.
[7] A. Ben-Naim, Statistical mechanics of waterlike particles in two dimensions. I. Physical model and application of the percus yevick equation, J. Chem. Phys. 54 (1971) 3682.
[8] A. Bizjak, T. Urbic, V. Vlachy, K. Dill, The three-dimensional Mercedes-Benz model of water, Acta Chim. Slov. 54 (2007) 532–537.
[9] D.T. Bowron, A. Filipponi, M.A. Roberts, J.L. Finney, Hydrophobic hydration and the formation of a clathrate hydrate, Phys. Rev. Lett. 81 (1998) 4164–4167.
[10] P. Bruscolini, L. Casetti, Lattice model for cold and warm swelling of polymers in water, Phys. Rev. E 61 (2000) R2208.
[11] P. Bruscolini, L. Casetti, Modeling hydration water and its role in polymer folding, J. Biol. Phys. 27 (2001) 243–256.
[12] S.V. Buldyrev, P. Kumar, H.E. Stanley, A physical mechanism underlying the increase of aqueous solubility of nonpolar compounds and the denaturation of proteins upon cooling, Conden. Mater. (2007). cond-mat/0701485.
[13] C. Buzano, E.D. Stefanis, M. Pretti, Low-temperature-induced swelling of a hydrophobic polymer: a lattice approach, J. Chem. Phys. 126 (7) (2007) 074904.
[14] H.S. Chan, K.A. Dill, Compact polymers, Macromolecules 22 (1989) 4559–4573.
[15] D. Chandler, Interfaces and the driving force of hydrophobic assembly, Nature 437 (2005) 640.
[16] S.K. Chandrayan, P. Guptasarma, Partial destabilization of native structure by a combination of heat and denaturant facilitates cold denaturation in a hyperthermophile protein, Proteins 72 (2008) 539.
[17] O. Collet, Warm and cold denaturation in the phase diagram of a protein lattice model, Europhys. Lett. 53 (2001) 93–99.
[18] O. Collet, Four-states phase diagram of proteins, Europhys. Lett. 72 (2005) 301–307.
[19] O. Collet, Folding kinetics of proteins and cold denaturation, J. Chem. Phys. 129 (15) (2008) 155101.
[20] S. Cooper, R. Dawber, History of cryosurgery, J. Roy. Soc. Med. 94 (2001) 196.
[21] T.E. Creighton, Protein folding, Biochem. J. 270 (1) (1990) 1–16.
[22] C. Dias, T. Ala-Nissila, M. Grant, M. Karttunen, Three-dimensional Mercedes-Benz model for water, J. Chem. Phys. 131 (2009) doi:10.1063/1.3183935.
[23] C.L. Dias, T. Ala-Nissila, M. Karttunen, I. Vattulainen, M. Grant, Microscopic mechanism for cold denaturation, Phys. Rev. Lett. 100 (2008) 118101.
[24] K.A. Dill, Dominant forces in protein folding, Biochemistry 29 (1990) 7133.
[25] K.A. Dill, T.M. Truskett, V. Vlachy, Hribar-Lee, Modeling water, the hydrophobic effect, and ion solvation, Annu. Rev. Biophys. Biomol. Struct. 34 (2005) 173.
[26] M. Doi, S.F. Edwards, The Theory of Polymer Dynamics, Oxford University Press, New York, 1988.
[27] J.T. Edsall, Apparent molal heat capacities of amino acids and other organic compounds, J. Am. Chem. Soc. 54 (1935) 1506–1507.
[28] S.E. Feller, Y. Zhang, R.W. Pastor, B.R. Brooks, Constant pressure molecular dynamics simulation: the langevin piston method, J. Chem. Phys. 103 (1995) 4613.

[29] A. Filipponi, D.T. Bowron, C. Lobban, J.L. Finney, Structural determination of the hydrophobic hydration shell of Kr, Phys. Rev. Lett. 79 (1997) 1293–1296.

[30] H.S. Frank, M.W. Evans, Free volume and entropy in condensed systems: III. Entropy in binary liquid mixtures; partial molal entropy in dilute solutions; structure and thermodynamics in aqueous electrolytes, J. Chem. Phys. 13 (1945) 507.

[31] S.J. Gill, S.F. Dec, G. Olofsson, I. Wadsoe, Anomalous heat capacity of hydrophobic solvation, J. Phys. Chem. 89 (1985) 3758.

[32] S.A. Hawley, Reversible pressure–temperature denaturation of chymotrypsinogen, Biochemistry 10 (1971) 2436–2442.

[33] F.G. Hopkins, Denaturation of proteins by urea and related substances, Nature 126 (1930) 383.

[34] G. Hummer, S. Garde, A.E. Garcia, M.E. Paulaitis, The pressure dependence of hydrophobic interactions is consistent with the observed pressure denaturation of proteins, Proc. Natl. Acad. Sci. USA 95 (1998) 1552.

[35] W. Kauzmann, Adv. Protein Chem. 14 (1959) 1.

[36] M. Kinoshita, T. Yoshidome, Molecular origin of the negative heat capacity of hydrophilic hydration, J. Chem. Phys. 130 (2009) 144705.

[37] R. Kitahara, A. Okuno, M. Kato, Y. Taniguchi, S. Yokoyama, K. Akasaka, Cold denaturation of ubiquitin at high pressure, Magn. Reson. Chem. 44 (2006) S108–S113.

[38] A. Kolb, B. Dünweg, Optimized constant pressure stochastic dynamics, J. Chem. Phys. 111 (1999) 4453.

[39] R. Kumar, N. Prakash Prabhu, K. Krishna Rao, K. Bhuyan, Abani, The alkali molten globule state of horse ferricytochrome *c*: observation of cold denaturation, J. Mol. Biol. 364 (2006) 483.

[40] S. Kunugi, N. Tanaka, Cold denaturation of proteins under high pressure, Biochim. Biophys. Acta 1595 (2002) 329–344.

[41] B. Lee, G. Graziano, A two-state model of hydrophobic hydration that produces compensation enthalpy and entropy changes, J. Am. Chem. Soc. 118 (22) (1996) 5163.

[42] Y. Li, B. Shan, D. Raleigh, The cold denatured state is compact but expands at low temperatures: hydrodynamic properties of the cold denatured state of the c-terminal domain of l9, J. Mol. Biol. 368 (2007) 256.

[43] J. Liang, K.A. Dill, Are proteins well-packed?, Biophys. J. 81 (2001) 751.

[44] J.R. Livingstone, R.S. Spolar, M.T. Record, Contribution to the thermodynamics of protein folding from the reduction in water-accessible nonpolar surface area, Biochemistry 30 (1991) 4237.

[45] M.I. Marques, J.M. Borreguero, H.E. Stanley, N.V. Dokholyan, Possible mechanism for cold denaturation of proteins at high pressure, Phys. Rev. Lett. 91 (13) (2003) 138103.

[46] F. Meersman, C.M. Dobson, K. Heremans, Protein unfolding, amyloid fibril formation and configurational energy landscapes under high pressure conditions, Chem. Soc. Rev. 35 (2006) 908–917.

[47] S. Melchionna, G. Briganti, P. Londei, P. Cammarano, Water induced effects on the thermal response of a protein, Phys. Rev. Lett. 92 (15) (2004) 158101.

[48] S. Moelbert, B. Normand, P.D.L. Rios, Kosmotropes and chaotropes: modelling preferential exclusion, binding and aggregate stability, Biophys. Chem. 112 (2004) 45.

[49] S. Moelbert, P.D.L. Rios, Chaotropic effect and preferential binding in a hydrophobic interaction model, J. Chem. Phys 119 (15) (2003) 7988–8001.

[50] N. Muller, Search for a realistic view of hydrophobic effects, Acc. Chem. Res. 23 (1990) 23–28.

[51] A. Nicholls, K.A. Sharp, B. Honig, Protein folding and association: insights from the interfacial and thermodynamic properties of hydrocarbons, Proteins 11 (1991) 281.

[52] C.N. Pace, C. Tanford, Thermodynamics of the unfolding of b-lactoglobulin a in aqueous urea solutions between 5 and 55 °C, Biochemistry 7 (1968) 198.

[53] G. Panick, G.J.A. Vidugiris, R. Malessa, G. Rapp, R. Winter, C. Royer, Exploring the temperature–pressure phase diagram of staphylococcal nuclease, Biochemistry 38 (1999) 4157–4164.

[54] D. Paschek, S. Nonn, A. Geiger, Low-temperature and high-pressure induced swelling of a hydrophobic polymer-chain in aqueous solution, Phys. Chem. Chem. Phys. 7 (2005) 2780–2786.

[55] B.A. Patel, P.G. Debenedetti, F.H. Stillinger, P.J. Rossky, The effect of sequence on the conformational stability of a model heteropolymer in explicit water, J. Chem. Phys. 128 (2008) 175102.

[56] N.V. Prabhu, K.A. Sharp, Heat capacity in proteins, Annu. Rev. Phys. Chem. 56 (2005) 521.

[57] P.L. Privalov, Thermodynamics of protein folding, J. Chem. Thermodyn. 29 (1997) 447–474.

[58] P.L. Privalov, Y.V. Griko, S.Y. Venyaminov, Cold denaturation of myoglobin, J. Mol. Biol. 190 (1986) 487–498.

[59] R. Ravindra, R. Winter, On the temperature–pressure free-energy landscape of proteins, ChemPhysChem 4 (2003) 359–365.

[60] T.R. Rettich, Y.P. Handa, R. Battino, E. Wilhelm, Solubility of gases in liquids. 13. High-precision determination of Henry's constants for methane and ethane in liquid water at 275–328 K, J. Phys. Chem. 85 (1981) 3230.

[61] P.D.L. Rios, G. Caldarelli, Putting proteins back into water, Phys. Rev. E 62 (2000) 8449.

[62] P.D.L. Rios, G. Caldarelli, Cold and warm swelling of hydrophobic polymers, Phys. Rev. E 63 (2001) 031802.

[63] A.D. Robertson, K.P. Murphy, Protein structure and the energetics of protein stability, Chem. Rev. 97 (1997) 1251.

[64] T. Róg, K. Murzyn, J. Milhaud, M. Karttunen, M. Pasenkiewicz-Gierula, Water isotope effect on the bilayer properties: a molecular dynamics simulation study, J. Phys. Chem. B 113 (2009) 97.

[65] G. Salvi, S. Molbert, P.D.L. Rios, Design of lattice proteins with explicit solvent, Phys. Rev. E 66 (2002) 061911.

[66] K.A.T. Silverstein, A.D.J. Haymet, K.A. Dill, A simple model of water and the hydrophobic effect, J. Am. Chem. Soc. 120 (13) (1998) 3166–3175.

[67] K.A.T. Silverstein, A.D.J. Haymet, K.A. Dill, Molecular model of hydrophobic solvation, J. Chem. Phys. 111 (17) (1999) 8000–8009.

[68] L. Smeller, Pressure–temperature phase diagrams of biomolecules, Biochim. Biophys. Acta 1595 (2002) 11–29.

[69] N.T. Southall, K.A. Dill, Potential of mean force between two hydrophobic solutes in water, Biophys. Chem. 101–102 (2002) 295–307.

[70] T. Yoshidome, M. Kinoshita, Hydrophobicity at low temperatures and cold denaturation of a protein, Phys. Rev. E 79 (3) (2009) 030905.

[71] A. Zipp, W. Kauzmann, Pressure denaturation of metmyoglobin, Biochemistry 12 (1973) 4217–4228.